

The Interaction of Baccatin III with the Taxol Binding Site of Microtubules Determined by a Homogeneous Assay with Fluorescent Taxoid[†]

Jose M. Andreu* and Isabel Barasoain

Centro de Investigaciones Biológicas, CSIC, Velazquez 144, 28006 Madrid, Spain

Received April 27, 2001; Revised Manuscript Received July 20, 2001

ABSTRACT: The ubiquitous Taxol binding site of microtubules also binds newly discovered ligands. We have designed a homogeneous assay for the high throughput detection of Taxol biomimetics, based on the displacement of 7-*O*-[*N*-(2,7-difluoro-4'-fluoresceincarbonyl)-*L*-alanyl]Taxol from its binding site in diluted solutions of preserved microtubules. The state of this reference ligand is measured by fluorescence anisotropy in a microplate reader, with varying concentrations of nonfluorescent competitors. The binding equilibrium constant of Taxol has a value $K_b = 3.7 \times 10^7 \text{ M}^{-1}$. We have found that baccatin III, an analogue of Taxol without the C-13 side chain, binds with $K_b = 1.5 \times 10^5 \text{ M}^{-1}$, whereas the side chain methyl ester is inactive. This was unexpected from the structure–activity relationship of taxoids but compatible with models of Taxol docked at the microtubule site. Baccatin III binding has been confirmed by displacement of [³H]Taxol and by direct HPLC measurements of its cosedimentation with microtubules, among other methods. Consequently, baccatin III induces microtubule bundles and multipolar spindles in PtK2 and U937 cells, and mitotic arrest and apoptotic death of the U937 cells, at concentrations 200–500-fold larger than Taxol. The simplest analysis of these results strongly suggests that the interaction of the C-2 C-4 substituted taxane ring system with the microtubule binding site provides most (ca. 75%) of the free energy change of Taxol binding and is sufficient to activate microtubule stabilization and transmit the antitumor effects of Taxol, whereas the C-13 side chain provides a weak specific anchor.

Taxol, a plant diterpenoid widely employed in cancer chemotherapy, promotes $\alpha\beta$ -tubulin assembly by binding to β -tubulin in microtubules. Its effect is related to that of the GTP¹ nucleotide, with important differences. GTP binds at one end of the tubulin dimer, making contact with the next dimer along each protofilament forming the microtubule, whereas Taxol binds at one side of β -tubulin near the contact with the next protofilament; in α -tubulin, the zone corresponding to the Taxol binding cavity is occupied by a loop of the peptide chain (1). Unassembled tubulin dimers bind GTP, and the binding site gets buried by assembly, whereas the Taxol binding site is only conformed in assembled tubulin. The hydrolysis of GTP permits disassembly and the regulation of the microtubule system; however, the activation of tubulin by Taxol is permanent, stabilizing the microtubules.

Suppression of the cellular microtubule dynamics by Taxol is a main cause of the inhibition of cell division and of tumor

cell death (2). A number of diverse natural substances, including epothilones (3), discodermolide (4), eleutherobin (5), and laulimalide (6), mimic the cytotoxic effects of Taxol, apparently by binding to its ubiquitous microtubule site. Each of these substances was discovered with typically different assays or screens for Taxol-like activities. In contrast with other important biological targets, at this stage there is a lack of a standard assay to directly detect and measure the binding of other ligands to the Taxol binding site of microtubules. Luminescence-based methods would be very useful for these purposes. Active, water-soluble, fluorescent derivatives of Taxol attached with an alanine spacer at nonessential position 7 (7) are specific probes of the Taxol binding site of microtubules (8). These fluorescent taxoids have been mainly employed to locate subcellular sites of cytotoxic taxoid binding to spindle pole microtubules and to centrosomes (9), as well as for measuring the fast kinetics of binding to and dissociation from the Taxol site, which is exposed in microtubules (10). A first proposal of the present work was to develop a homogeneous fluorescent assay of ligand binding to the Taxol site of microtubules, with the goal of facilitating high throughput detection of new Taxol mimetics.

On the other hand, numerous structure–activity studies have been performed with Taxol analogues (11–15). The side chain at position C-13 and the taxane ring system have been regarded as essential determinants for the activity of Taxol and docetaxel. The isolated side chain and the taxane ring system with its other substituents, exemplified by baccatin III, have generally been considered inactive on

[†] This work was supported by MCyT Grant BIO2000-0748 and Programa de Grupos Estratégicos de la Comunidad de Madrid.

* To whom correspondence should be addressed. E-mail: j.m.andreu@cib.csic.es. Fax: +34 91 5627518. Phone: +34 91 51611800.

¹ Abbreviations: GTP, guanosine 5'-triphosphate; GDP, guanosine 5'-diphosphate; DMSO, dimethyl sulfoxide; EGTA, ethylene glycol bis-(β -aminoethyl ether)-*N,N,N',N'*-tetraacetic acid; GAB buffer, 10 mM sodium phosphate, 1 mM EGTA, 0.1 mM GTP, 6 mM MgCl₂, 3.4 M glycerol, pH 6.5; Flutax-2, 7-*O*-[*N*-(2,7-difluoro-4'-fluoresceincarbonyl)-*L*-alanyl]Taxol; PBS, phosphate-buffered saline; Hepes, *N*-(2-hydroxyethyl)piperazine-*N'*-2-ethanesulfonic acid; RET, resonance energy transfer.

mammalian microtubules, although baccatin III stabilized *Physarum* microtubules against cold-induced disassembly (11) and conflicting reports about its antimitotic activity on different cell lines can be found (16–19, 22). However, several molecular docking models of bound Taxol have recently been presented, which include extensive contacts of the 2-*O*-benzoyl and the taxane ring system with several residues in the structure of β -tubulin. These models are supported by experimental evidence coming from photoaffinity labeling (20), fluorescence and REDOR NMR spectroscopy (21), the activity of 2-*m*-azido-baccatin III (19), and point mutations conferring Taxol or epothilone resistance (22) or by careful conformational analysis in correlation with the electron crystallographic density (23). In the present work it has been found that baccatin III can in fact replace Taxol at the microtubule binding site and mimic its effects. Analysis of baccatin and Taxol bindings suggests that most of the affinity of Taxol is contributed by the interaction of the 2-*O*-benzoyl-taxane ring system with the microtubule binding site, whereas the C-13 side chain provides only a specific additional anchor.

EXPERIMENTAL PROCEDURES

Taxoids. Stock solutions of taxoids were prepared in DMSO and kept dry at -20°C . Taxol was provided by the late M. Suffness from the National Cancer Institute (Bethesda, MD); it was measured spectrophotometrically at 273 nm after dilution in methanol, employing an extinction coefficient of $1700\text{ M}^{-1}\text{ cm}^{-1}$ (24). [^3H]Taxol (4 Ci mmol^{-1}) was from Moravek Biochemicals (Brea, CA). Docetaxel (Taxotere) was from Rhône-Poulenc Rorer (Antony, France). Baccatin III was from Sigma; it was found devoid of impurities by HPLC (a 20–80% gradient of acetonitrile in 0.05% aqueous trifluoroacetic acid, in a C-18 column, monitored at 228 nm). An approximately determined extinction coefficient of baccatin was $900 \pm 100\text{ M}^{-1}\text{ cm}^{-1}$ (273 nm, methanol). Baccatin III was soluble at the concentrations employed in 10 mM sodium phosphate, 1 mM EGTA, 0.1 mM GTP, 6 mM MgCl_2 , and 3.4 M glycerol, pH 6.5 (GAB buffer), containing 1% DMSO. The methyl ester of the C-13 side chain of Taxol was provided by E. Baloglu and D. G. I. Kingston from the Virginia Polytechnic Institute (Blacksburg, VA). The molar absorptivity of this compound was about $750\text{ M}^{-1}\text{ cm}^{-1}$ at 273 nm (absorption tail, methanol), and it was soluble to 0.75 mM in GAB buffer–1% DMSO. Note that the added 273 nm absorptivities of baccatin III and the side chain methyl ester approximately matched that of Taxol. Flutax-2 was provided by F. Amat-Guerri, Instituto de Quimica Organica, CSIC (Madrid, Spain); its purity was checked by HPLC, and its concentration was determined spectrophotometrically with 0.5% sodium dodecyl sulfate (SDS) at neutral pH, employing an extinction coefficient of $49\,100\text{ M}^{-1}\text{ cm}^{-1}$ at 496 nm (10).

Cross-Linked Microtubules. Bovine brain tubulin was purified and stored, and its concentration was measured as described (25). Prior to use it was equilibrated in 10 mM sodium phosphate, 1 mM EGTA, 0.1 mM GTP, and 3.5 M glycerol pH 6.8, with a cold Sephadex G-25 gravity column and centrifuged for 10 min at 50 000 rpm in a cold TLA100.4 rotor (Beckman). Tubulin (50 μM) was made 6 mM in MgCl_2 (that is, glycerol assembly buffer GAB, final pH 6.5) and 1

mM GTP, assembled into microtubules at 37°C , and gently cross-linked with 20 mM glutaraldehyde, quenched with NaBH_4 as described (10). These cross-linked microtubules have the same Flutax-2 binding stoichiometry, kinetics, and specificity as non-cross-linked controls; they have a normal morphology under the electron microscope (10). For this work, the cross-linked microtubules were dialyzed against GAB–0.1 mM GDP during $>36\text{ h}$ in the cold and stored at 4°C with 0.05% sodium azide (GDP substituted for GTP at this stage in order to have a chemically defined system upon prolonged storage). Their total tubulin concentration was measured after dilution in 1% SDS employing an extinction coefficient of $107\,000\text{ M}^{-1}\text{ cm}^{-1}$ at 275 nm (24). The concentration of assembled tubulin was determined by sedimentation and typically found to be 80% of total. The concentration of taxoid binding sites was determined by addition of increasing concentrations of cross-linked microtubules to 5 μM Flutax-2 in the GAB–GDP buffer, sedimentation (10 min, 50 000 rpm in a Beckman TLA120 rotor at 25°C), and spectrophotometric measurement of Flutax-2. The cross-linked microtubule preparations were found to bind 0.75 ± 0.05 Flutax-2 per total tubulin (i.e., about 95% of the assembled tubulin was active in binding this ligand). Control measurements employing [^3H]Taxol and scintillation counting gave values similar to those of Flutax-2. Once the anisotropy values of free and microtubule-bound Flutax had been determined, the number of sites could also be determined by titration of dilute cross-linked microtubule solutions with Flutax-2 (see below and Results). The concentration of taxoid binding sites of the cross-linked microtubule preparations was found to decay at rates comprised between 0.02 and 0.05 day^{-1} at 4°C (half-life of 5 and 2 weeks, respectively). Cross-linked microtubules were employed within one half-life from preparation. A fluorescence micrograph of cross-linked microtubules imaged with Flutax-2 is shown in Figure 1.

Fluorescence Spectroscopy and Anisotropy Measurements. Corrected fluorescence spectra were acquired with a photon counting Fluorolog-3-221 instrument (Jobin Yvon-Spex, Longjumeau, France), employing 1 nm excitation and 5 nm emission bandwidth, at 25°C . Fluorometric concentration measurements were made with a Shimadzu RF-540 spectrofluorometer. Anisotropy spectra and measurements were collected in the Fluorolog T-format mode with vertically polarized excitation and corrected for the sensitivity of each channel with horizontally polarized excitation (26). Multiple anisotropy measurements were practically made with a PolarStar microplate reader (BMG Labtechnologies, Offenburg, Germany) at 25°C . The solutions were excited with 200 flashes of vertically polarized light (485-P, 480–492 nm band-pass filter), and the emission was simultaneously analyzed with vertical and horizontal polarizing filters (520-P, 515–550 nm band-pass). The gain of the two channels was adjusted to give the anisotropy value of free Flutax-2 (0.055, polarization 0.080; GAB buffer at 25°C) in wells containing Flutax-2 and no microtubules. Blank values from wells with microtubules and no Flutax-2 were subtracted from the fluorescence intensity values (blanks typically represented less than 4% of the measurement).

Binding of Flutax to Microtubules. Flutax-2 (50 nM) was first titrated with increasing concentrations of binding sites provided by cross-linked microtubules in GAB buffer in a

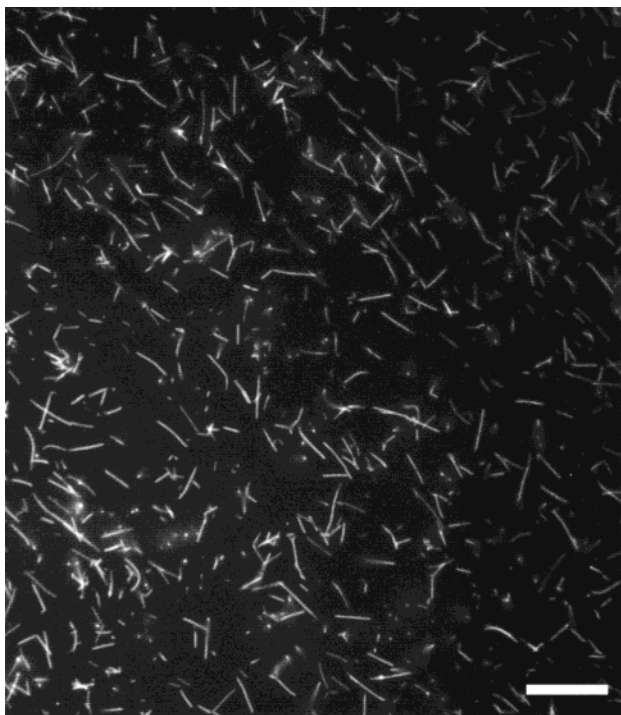


FIGURE 1: Fluorescence micrograph of a typical reaction mixture employed in this work, consisting of stabilized microtubules (100 nM taxoid sites) and fluorescent taxoid Flutax-2 (100 nM). The bar indicates 10 μm .

fluorescence cuvette at 25 °C. The fraction of Flutax-2 bound is

$$[F]_b/[F]_0 = (r - r_{\min})/(r_{\max} - r_{\min}) \quad (1)$$

where $[F]_b$ and $[F]_0$ are bound and total concentrations of Flutax-2 respectively, r is its fluorescence anisotropy measured with the spectrofluorometer, the value of r_{\min} is 0.055, and the value of r_{\max} was an adjustable parameter. Assuming a one to one binding, the concentration of free binding sites $[S]$ is

$$[S] = [S]_0 - [F]_b \quad (2)$$

and the following expression applies:

$$r = r_{\min} + (r_{\max} - r_{\min})K_b[S]/(1 + K[S]) \quad (3)$$

Equation 3 was iteratively applied to fit the r vs $[S]$ data, employing eqs 1 and 2 with different starting values of r_{\max} , with Sigmaplot (Jandel Scientific), from which a best fitted value was obtained: $r_{\max} = 0.29$. Control measurements with microtubule binding sites blocked by 10 μM Taxol gave r values very close to r_{\min} , within a $[S]_0$ range from 0 to 100 nM. Cross-linked microtubules (50–100 nM total tubulin) were then titrated with known concentrations of Flutax-2. The binding was determined as

$$[F]_b/[T]_0 = [F]_0(r - r_{\min})/[T]_0(r_{\max} - r_{\min}) \quad (4)$$

where $[T]_0$ is the total tubulin concentration and r_{\max} and r_{\min} have the previously determined values. The concentration of free Flutax-2 is

$$[F] = [F]_0 - [F]_b \quad (5)$$

The binding equation for independent sites

$$[F]_b/[T]_0 = nK_b[F]/(1 + K_b[F]) \quad (6)$$

was iteratively fitted to the data with Sigmaplot to obtain the best fitted values of n , the number of binding sites of Flutax-2 per total tubulin, and K_b , the binding equilibrium constant. When these procedures were repeated by employing the polarization plate reader, instead of the spectrofluorometer, smaller r_{\max} values of 0.245 (Costar 3599 plates) and 0.27 (Nunc 267342 black plates) and K_b and n values within experimental error were obtained.

Measurements of Ligand Binding to the Taxol Binding Site of Microtubules by Displacement of Flutax-2. These competitive measurements were made with the polarization plate reader. A solution of known concentrations of microtubule binding sites and Flutax-2, both close to 50 nM, in GAB-GDP buffer was freshly prepared from concentrated stocks of cross-linked microtubules and Flutax-2. It was dispensed in 200 μL aliquots (final volume) at room temperature in 96-well polystyrene plates (Costar catalog no. 3599; the border wells were not used). These plates were selected by checking that Flutax-2 remained in solution, instead of adsorbing to the plastic, measuring the contents of the wells with the spectrofluorometer (90% recovery). The ligands to be tested were added in small volumes of DMSO (final DMSO concentration 2% v/v) to make the desired duplicate concentrations. It was also checked that Taxol did not adsorb to the plate during the assay, employing $[^3\text{H}]$ Taxol and scintillation counting. Wells without protein and without Flutax-2 were included for calibration and background measurements, respectively (see anisotropy measurements above). The plates were rotary shaken for 10 min and measured twice within 30–90 min after equilibration at 25 °C in the microplate reader. The Flutax-2 anisotropy data were calculated with the evaluation software (BMG-Excel) and plotted versus total competitor concentration.

To measure the binding affinity of a ligand (L) displacing the reference ligand Flutax-2 (F) from its microtubule binding site (S), unitary stoichiometry was assumed, the fractional binding of Flutax-2 was determined from the anisotropy as

$$[F]_b/[S]_0 = [F]_0(r - r_{\min})/[S]_0(r_{\max} - r_{\min}) \quad (7)$$

and the following expressions were applied:

$$K(F) = [SF]/[S][F] \quad (8)$$

$$K(L) = [SL]/[S][L] \quad (9)$$

$$[F] = [F]_0 - [SF] \quad (10)$$

$$[L] = [L]_0 - [SL] \quad (11)$$

$$[S] = [S]_0 - [SL] - [SF] \quad (12)$$

A personal computer program, implementing the solution to eqs (8–12) from the known values of $[F]_0$, $[L]_0$, $[S]_0$, and $K(F)$, was employed to find the best least-squares fit value of the equilibrium binding constant of the competing ligand $K(L)$ to the $[F]_b/[S]_0$ versus $[L]_0$ data (27; J. F. Diaz, unpublished program Equigra.4). The fitted displacement curve was expressed as anisotropy and plotted with the data.

Displacement of [^3H]Taxol from Microtubules by Competing Ligands. [^3H]Taxol (100 nM), 100 nM microtubule binding sites, and the desired concentration of competitor in a final volume of 200 μL of GAB-GDP buffer containing 1 mg mL^{-1} bovine serum albumin (BSA) and 1% DMSO were incubated for 30 min and centrifuged for 10 min at 50 000 rpm, 25 $^{\circ}\text{C}$, in polycarbonate tubes in a TLA100 rotor with a TLX tabletop ultracentrifuge (Beckman, Palo Alto, CA). The supernatants and the tubes containing the pellets were separated and counted with a liquid scintillation counter. The data could be numerically treated similarly to the above section, substituting Taxol for Flutax-2.

Binding of Baccatin III to Microtubules. Microtubule-bound baccatin III was measured by sedimentation and methanol extraction of the dried pellets, as for Taxol (24), followed by HPLC (see taxoids section above).

Fluorescence Microscopy and Flow Cytometry Methods. U937 monocytic human leukemia and PtK2 potoroo epithelial-like kidney cells were grown, and cytoskeletons were prepared as described (28). PtK2 cells were fixed with 3.7% formaldehyde, methanol, and acetone, U937 cytoskeletons were fixed with 3.7% formaldehyde, and indirect tubulin immunofluorescence (28) was performed with an additional 30 min incubation with 0.05 $\mu\text{g mL}^{-1}$ Hoechst 33342 to stain chromatin. Cells and cytoskeletons were observed through a 100 \times Plan-Apochromat objective with a Zeiss Axioplan epifluorescence microscope, and the images were recorded with a Hamamatsu 4742-95 cooled CCD camera (9).

Progression through the cell cycle was assessed by flow cytometry DNA determination with propidium iodide. Cells (300 000 per mL) were incubated with the drugs (U937 cells, 17 h; PtK2, 24 h). Cells were washed in PBS and fixed in 70% ethanol at 4 $^{\circ}\text{C}$ for 1 h, washed twice in phosphate-buffered saline (PBS), and resuspended in 500 μL of PBS containing 60 $\mu\text{g mL}^{-1}$ DNase-free RNase A and 50 $\mu\text{g mL}^{-1}$ propidium iodide. The samples were incubated at 37 $^{\circ}\text{C}$ for 30 min and analyzed with a Coulter Epics XL flow cytometer.

To determine cell death, U937 cells were washed with PBS and incubated for 15 min at room temperature in the dark in 100 μL of 10 mM HEPES, 150 mM NaCl, and 2.5 mM CaCl_2 , pH 7.4, containing 5 μL of fluorescein isothiocyanate-conjugated annexin V (Molecular Probes, Eugene, OR) and 1 μg propidium iodide (PI). After incubation, 400 μL of the same buffer was added, and the cells were analyzed by flow cytometry using appropriate color filters to determine the propidium iodide-derived reddish orange fluorescence (590 nm) and the fluorescein-derived greenish fluorescence (530 nm). Apoptotic cells were characterized by annexin V binding but with null or low propidium iodide influx, whereas necrotic cells were characterized by annexin V binding and a large increase in red fluorescence because of the massive influx of PI (29).

RESULTS AND DISCUSSION

To set up an efficient fluorescence-based competitive assay for ligand binding to the Taxol site of microtubules, the changes of the fluorescent properties of the probe 7-*O*-[*N*-(2,7-difluoro-4'-fluoresceincarbonyl)-*L*-alanyl]Taxol (Flutax-2; 10) upon specific binding to microtubules were further investigated. Flutax-2 was preferred over the nonfluorinated

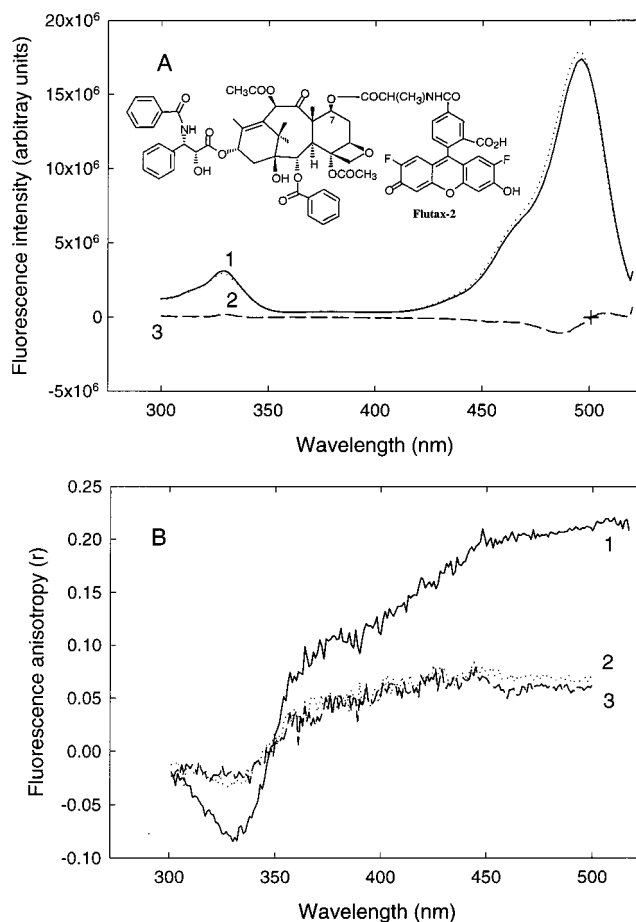


FIGURE 2: (A) Fluorescence excitation spectra of 50 nM Flutax-2 in GAB-GDP buffer at 25 $^{\circ}\text{C}$: 1 (continuous line), with 50 nM microtubule binding sites; 2 (dotted line), free Flutax-2; 3 (dashed line), difference spectrum generated by subtracting spectrum 2 from spectrum 1 (the cross-hair marks an isosbestic point at 500 nm). (B) Fluorescence anisotropy excitation spectra of 50 nM Flutax-2 under the same conditions. 1 (continuous line), with 50 nM microtubule binding sites; 2 (dotted line), with 50 nM microtubule binding sites and 10 μM Taxol or 1 mM baccatin III; 3 (dashed line), free Flutax-2. Each of these anisotropy spectra is the average of two (5 s photon counting interval, 1 nm step size). Spectrum 2 is the average of the two identical spectra obtained with Taxol and baccatin. Spectrum 3 is the average of two identical spectra acquired with and without 10 μM Taxol.

fluorescein analogue Flutax-1 for its superior photostability and acidic pK (giving the strongly fluorescent dianion at neutral pH values). Fluorescence anisotropy and resonance energy transfer (RET) methods were explored, instead of emission intensity measurements (with Flutax-1). Since microtubules bind Taxol and Flutax with high affinity, low concentrations of binding sites are needed in order to detect lower affinity competitors. These dilution-stabilized binding sites were provided by gently cross-linked microtubules (Figure 1 and Experimental Procedures; 8, 10).

Measurement of Specific Flutax-2 Binding to Microtubules with Fluorescence Anisotropy. The fluorescence intensity of Flutax-2 changes very little upon binding to microtubules. There is a small shift in the excitation maximum from 494 to 495 nm (excitation spectra, Figure 2A; isosbestic point at 500 nm) and an emission blue shift from 523 to 520 nm (emission spectra are not shown; isosbestic point at 525 nm; see ref 10). The fluorescence polarization of Flutax-2 increases upon binding. Figure 2B shows the excitation

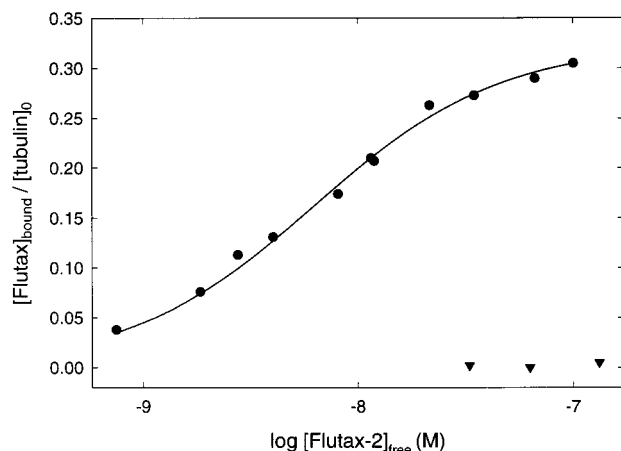


FIGURE 3: Isotherm of binding of Flutax-2 to stabilized microtubules in GAB-GDP buffer at 25 °C, determined from the change in fluorescence anisotropy of the ligand (excitation 495 nm, emission 520 nm). The solid circles are the binding measurements and the inverted triangles specificity controls in which the binding sites were blocked with 10 μ M Taxol. The solid line is a best fitting binding curve, with a binding equilibrium constant $K_b = 1.5 \times 10^8 \text{ M}^{-1}$ and the number of sites $n = 0.33$ per total tubulin. The total concentration of tubulin was 100 nM, and the cross-linked microtubule preparation had been stored for 20 days at 4 °C. This preparation initially bound 0.8 Flutax-2 per assembled tubulin (60% of total) and decayed at a rate of 0.02 site per day.

anisotropy spectrum of a 50 nM Flutax-2-microtubule site solution (trace 1) in comparison with the spectrum of a similar solution in which the binding sites were blocked with a Taxol excess (trace 2) and that of free Flutax-2 (trace 3). Both the negative anisotropy of the 329 nm band and the positive anisotropy of the lower energy (495 nm) excitation transition of the difluorofluorescein are specifically enlarged by Flutax-2 binding to microtubules. The anisotropy values determined for the 495 nm band (emission 520 nm; glycerol-containing GAB buffer, 25 °C) were as follows: free Flutax-2 (50 nM), $r_{\min} = 0.055$; in the presence of microtubules blocked with Taxol, $r = 0.060$; Flutax-2 specifically bound to microtubules, $r_{\max} = 0.29$ (the latter was determined by titration of 50 nM Flutax-2 with increasing microtubule concentrations). These changes are consistent with a strong immobilization of the fluorophore upon binding. In addition to anchoring Flutax-2 through its Taxol moiety, an interaction of the fluorescein dianion with a cationic residue of microtubules, possibly Arg282 of β -tubulin, has been proposed (8; see Figure 10 in ref 10).

A binding isotherm of Flutax-2 to microtubules, determined from the change of ligand anisotropy, is shown by Figure 3. The binding equilibrium constant has a value $K_b = (1.5 \pm 0.4) \times 10^8 \text{ M}^{-1}$ in GAB-GDP buffer at 25 °C [from Figure 3 and the titration of Flutax-2 with microtubule sites; this is not significantly different from values previously determined by centrifugation (10)]. The binding of Flutax-2 at these concentrations is completely abolished by 10 mM Taxol (Figure 3). On the basis of these results, the ability of Flutax-2 to replace [^3H]Taxol from its binding site (see Figure 5 below), and previous results discussed in a detailed kinetic study (10), Flutax-2 can be considered a bona fide probe of the Taxol binding site of microtubules.

Resonance Energy Transfer (RET) between Microtubule-Bound Fluorescent Taxoids. The lateral distance between Taxol binding sites in neighbor β -tubulin subunits of

microtubules (ca. 5 nm; 30) is suitable for RET from fluorescein to rhodamine fluorophores (Förster distance R_0 5.5 nm). Displacement of the donor or acceptor from their binding sites by another nonfluorescent ligand should suppress the emission of the acceptor upon donor excitation. The emission spectrum (excitation at 460 nm) of 50 nM microtubule binding sites with 10 nM Flutax-2 and 40 nM Rotax [7-*O*-[*N*-(4'-tetramethylrhodaminecarbonyl)-*L*-alanyl]-Taxol (8)] showed a peak of sensitized Rotax emission in addition to the emission of Flutax-2 (not shown). When the binding sites were blocked with Taxol, the fluorescein emission increased (was not quenched) and shifted from 521 to 524 nm, whereas the rhodamine contribution decreased to a level (a shoulder) which was similar to that of the unsensitized emission of Rotax at 582 nm. This experiment indicated the feasibility of detecting a ligand binding to the Taxol site by the decrease of RET, although with a relatively small signal change.

A Competitive Fluorescent Assay of Ligand Binding to Microtubules Measures the Binding of Taxol and Baccatin III. Employing Flutax-2 as a reference ligand of the Taxol binding site, the binding of other nonfluorescent ligands displacing Flutax-2 can be more easily measured by the changes in its own fluorescence properties. In this work the signal employed was the large change in fluorescence anisotropy, which was practically screened in 96-well plates with a microplate reader. Figure 4 shows how Taxol and docetaxel efficiently decrease the fluorescence anisotropy of solutions of 50 nM Flutax-2-50 nM microtubule sites. Numerical analysis of the displacement isotherms (Experimental Procedures) indicated that Taxol and docetaxel bind to microtubules with equilibrium binding constants of $(3.7 \pm 1.5) \times 10^7 \text{ M}^{-1}$ (four determinations) and $(6.0 \pm 2.3) \times 10^7 \text{ M}^{-1}$ (two determinations), respectively (25 °C). The affinity ratio of docetaxel to Taxol was 2.7 ± 0.2 from individual experiments. A 2-fold larger affinity of docetaxel compared with Taxol agrees with a previous direct determination (24). The affinity of Taxol is in the same order of magnitude as previously determined values for Taxol (31), 2-debenzoyl-2-(*m*-aminobenzoyl)-Taxol (32), and 3'-*N*-(*m*-aminobenzamido)-3'-*N*-debenzamido-Taxol (33). Baccatin III, usually regarded as an inactive compound (see the introduction), was employed as a supposedly negative control in the competitive assay. Quite amazingly, baccatin III completely inhibited the Flutax-2-microtubule anisotropy, although at total concentrations roughly 200 larger than Taxol (Figure 4).

Analysis of the displacement data indicated that baccatin III is recognized by the Taxol binding site of microtubules with an equilibrium constant of $(1.5 \pm 0.5) \times 10^5 \text{ M}^{-1}$ (seven determinations). Baccatin III is equivalent to the taxane ring system, in which the C-13 OH group replaces the Taxol side chain (see chemical structures in Figure 4). On the other hand, the C-13 side chain has previously been regarded as an also essential determinant for the recognition of Taxol (see the introduction). However, the methyl ester of the C-13 side chain was, within its solubility limit, inactive in displacing Flutax-2. The results indicated a binding equilibrium constant below 10^3 M^{-1} for this analogue of the C-13 side chain separated from the rest of the molecule (Figure 4; two determinations).

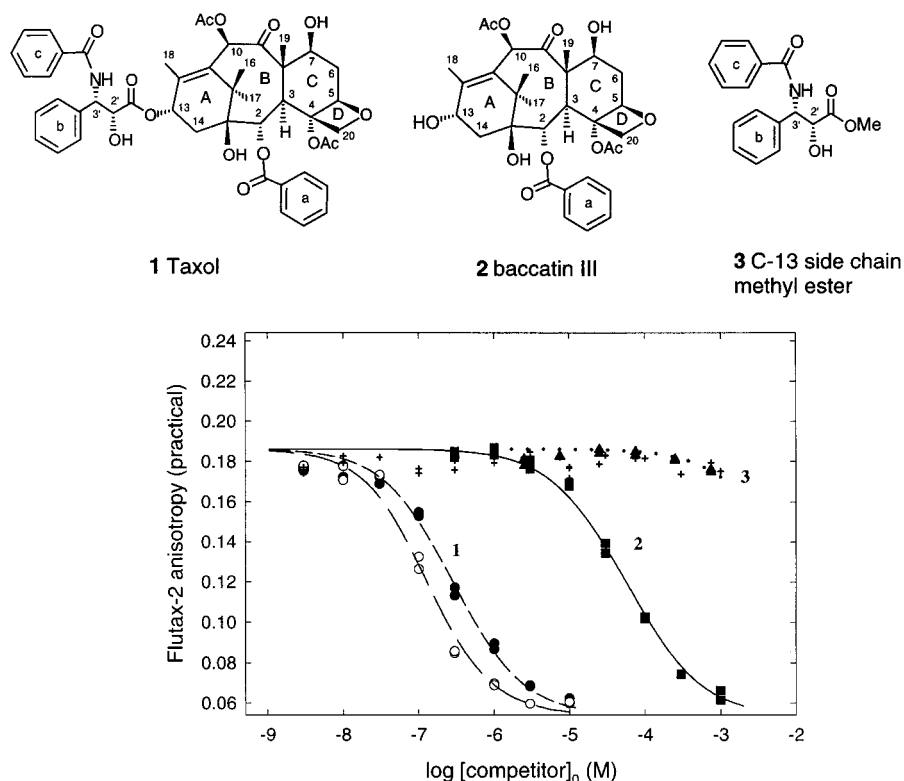


FIGURE 4: Competition isotherms of ligands binding to the Taxol site of microtubules in GAB-GDP buffer at 25 °C. The fluorescence anisotropy of multiple solutions of 50 nM Flutax-2 and 50 nM microtubule binding sites with diverse competitor concentrations was measured in duplicate, employing a microplate reader. Symbols: solid circles, Taxol (1); empty circles, docetaxel; squares, baccatin III (2); triangles, methyl ester of the Taxol C-13 side chain (3); cross-hairs, corresponding controls containing 1% (v/v) DMSO without ligand. In this experiment, each competition curve starts with an anisotropy value corresponding to two-thirds of the Flutax-2 molecules bound, which is progressively reduced by the competitor replacing Flutax-2 in the binding sites. The equilibrium binding constant of Flutax-2 is $1.5 \times 10^8 \text{ M}^{-1}$ (Results and Figure 3). Lines 1 (short dash) and 2 (solid) correspond to best fits (Experimental Procedures) for the binding of Taxol and baccatin to the same site with equilibrium constant values of $K = 3.2 \times 10^7 \text{ M}^{-1}$ and $K = 1.5 \times 10^5 \text{ M}^{-1}$ respectively; the long dashed line is the fit to the docetaxel data, $K = 8 \times 10^7 \text{ M}^{-1}$; the dotted line passing through the side chain methyl ester data is a simulation of a low-affinity binding with $K = 7 \times 10^2 \text{ M}^{-1}$ (note that these data are similar to the controls).

In view of these results, the rest of this study was dedicated to validating the interaction of baccatin III with microtubules detected with the multiwell plate assay, as well as assessing the relative contributions of the taxane ring system and the C-13 side chain to the affinity of Taxol recognition by microtubules and to the induction of the cellular effects of Taxol binding. It was first confirmed that baccatin III reduced the anisotropy excitation spectrum of Flutax-2 to that of the free probe (see Figure 2B, trace 2). In a kinetic experiment, fluorescence anisotropy was then employed to monitor the time course of displacement of Flutax-2 from its microtubule binding site by excess baccatin. The anisotropy decay could be fitted to a single exponential with a rate constant $k = 0.004 \text{ s}^{-1}$ at 25 °C (not shown), within a factor of 2 from the dissociation rate of Flutax-2 previously determined by displacement with docetaxel (0.007 s^{-1} ; 10).

In a series of control measurements, the displacement of the interaction of [^3H]Taxol with microtubules by baccatin III and Flutax-2 was evidenced by sedimentation and scintillation counting. The results of these measurements (Figure 5 and legend) are compatible with those of the fluorescence anisotropy assays, except for a 7-fold lower apparent affinity of Flutax-2. This confirmed that baccatin III is recognized by the Taxol binding site of cross-linked microtubules. However, to have most of the [^3H]Taxol tracer in solution, instead of sticking to the polycarbonate tube of the tabletop ultracentrifuge, it was necessary to include 1

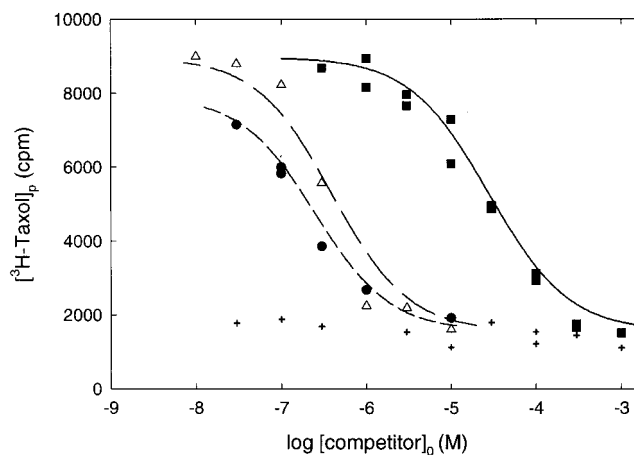


FIGURE 5: Displacement of [^3H]Taxol (100 nM total concentration) from microtubule binding sites (100 nM total concentration) by competing ligands in GAB-GDP buffer containing 1 mg/mL BSA at 25 °C. The counts per minute cosedimenting with microtubules are plotted versus competitor concentration (100 nM Taxol gave 18 000 cpm). Symbols: solid circles, unlabeled Taxol; triangles, Flutax-2; solid squares, baccatin III; cross hairs, controls of nonspecific sedimentation of [^3H]Taxol without microtubules. The solid line is a numerical best fit to the baccatin data (Experimental Procedures and Figure 4), assuming a [^3H]Taxol binding equilibrium constant of $K = 3.7 \times 10^7 \text{ M}^{-1}$ and yielding for baccatin III $K = 1.6 \times 10^5 \text{ M}^{-1}$. The long dashed line corresponds to a value of $K = 1.5 \times 10^7 \text{ M}^{-1}$ for Flutax-2 and the short dashed line to $K = 2.5 \times 10^7 \text{ M}^{-1}$ for the unlabeled Taxol.

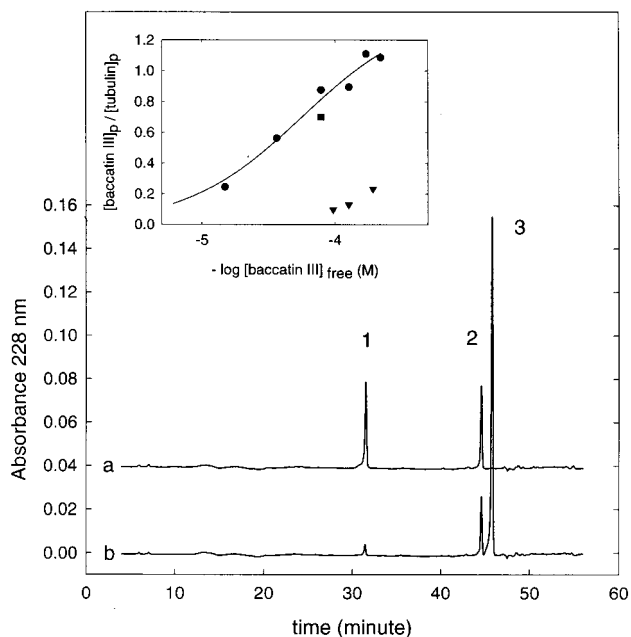


FIGURE 6: Direct identification and measurement of baccatin III binding to microtubules. Trace a is a HPLC analysis of the microtubule pellet from a solution containing 120 μM baccatin III and 41 μM cross-linked microtubule sites in GAB-GDP buffer at 25 $^{\circ}\text{C}$. Peak 1 is microtubule-bound baccatin III, peak 2 is 20 μM docetaxel added to the pellet as an internal standard. Trace b is a parallel sample to which 40 μM Taxol (peak 3) was added together with baccatin III. Inset: sedimentation-HPLC measurements of baccatin binding to native microtubules in GAB-1 mM GTP buffer at 37 $^{\circ}\text{C}$ (total tubulin concentration 30.5 μM). Symbols: circles, baccatin III binding (the solid line is an approximate fit with an equilibrium constant $K_b = 1.8 \times 10^4 \text{ M}^{-1}$ to 1.4 binding sites per assembled tubulin dimer); triangles, controls of nonspecific baccatin III binding made with 30 μM Taxol; square, one measurement of binding to cross-linked microtubules, simply shown for comparison.

mg mL⁻¹ BSA, which binds Taxol (keeping it available for interaction with microtubules) as well as Flutax-2 (lowering its apparent affinity). These adsorption processes precluded a direct rigorous measurement of the affinity of Taxol binding to microtubules in our hands and, hence, of the affinity of its competitors employing Taxol as a reference ligand in these diluted assays. Additional disadvantages of the [³H]Taxol binding assays in comparison with the homogeneous fluorescent taxoid anisotropy assay are the centrifuging, separation, and radioactive counting operations required.

Baccatin III Binds to and Stabilizes Microtubules Assembled from Purified Tubulin. Still concerned by the possibility that the effects observed could be due to a minor contaminant of highly active taxoid in the baccatin employed (or a result of using cross-linked microtubules), we sought direct proof of the interaction of baccatin III with microtubules. It was first observed that baccatin (200 μM) induced full microtubule assembly from a purified tubulin solution below the critical protein concentration for assembly (GAB-GTP at 37 $^{\circ}\text{C}$; not shown), in agreement with Chatterjee et al. (34). This is a property characteristic of active taxoid interaction with microtubules (24). Microtubule-bound baccatin III could actually be identified and quantified by cosedimentation and HPLC. Figure 6 shows the results of one experiment in which the binding of 0.70 baccatin molecules per site of cross-linked microtubules (Figure 6, trace a, peak 1) was reduced to 0.13 baccatin per site by

Taxol (Figure 6, trace b). Native (non-cross-linked) microtubules similarly bound baccatin III with a stoichiometry of specific binding near one baccatin per assembled tubulin dimer (inset to Figure 6; the apparent binding equilibrium constant is roughly $1.8 \times 10^4 \text{ M}^{-1}$, but note that this is not a rigorous measurement since the ligand binding pulled additional tubulin into assembly).

Baccatin III Competes with Flutax-2 for in Situ Binding to Cellular Microtubules. It was of interest to know whether the interaction of baccatin with the Taxol binding site of microtubules assembled from purified tubulin would also hold for cellular microtubules. Flutax-2 (200 nM) stains the native microtubules of unfixed PtK2 cytoskeletons, which are directly imaged by epifluorescence microscopy (Figure 7A). Addition of 500 nM Taxol erases the images of most cytoplasmic microtubules, while the stronger labeling of centrosomes and spindle pole microtubules persists (Figure 7B). Addition of 100 mM baccatin III has a very similar effect (Figure 7C). Addition of larger concentrations of baccatin III or Taxol fully erases the microtubule cytoskeletal images (Figure 7D, 1 mM baccatin). These results provide visual confirmation that baccatin III binds to the Taxol site of microtubules, albeit at a several 100-fold larger concentration than Taxol.

Baccatin III Induces Abnormal Mitotic Spindles, Microtubule Bundles, and Human Leukemia Cell Death. Centrosomes and spindle pole microtubules, whose Flutax-2 images are erased at the last by baccatin III and Taxol (Figure 7), are subcellular targets of cytotoxic taxoid binding (9). In view of these results (and the conflicting reports on the cytotoxicity of baccatin III, see the introduction), we questioned if baccatin III would be able to induce the characteristic cellular effects of Taxol. The effects of baccatin III (0.1–0.5 mM) on PtK2 cells consisted of a disorganization in the cytoplasmic microtubule networks relative to control cells, the appearance of microtubule bundles and lobulated nuclei (Figure 8D), and characteristic multipolar spindles (Figure 8 E,F), similar to the effects of 5 μM Taxol on the same cells (not shown). U937 human promonocytic leukemia cells are much more sensitive to Taxol (9). Treatment of U937 cells (see control cells in Figure 8G–I) with 2.5 μM baccatin (17 h) induced microtubule bundles and apoptotic chromatin images (Figure 8J,K), as well as abnormal and multipolar mitosis (Figure 8L,M). These U937 cell lesions were similarly induced with 5 nM Taxol, whereas the 100 μM C-13 side chain methyl ester was inactive (not shown).

Baccatin III (2.5 μM) and Taxol (5 nM), but not the C-13 side chain methyl ester (100 μM), induced U937 cell cycle arrest in G₂-M and an accumulation of cells with sub-G₁ DNA content. Cell death was evidenced by the apoptotic translocation of plasma membrane phosphatidylserine, detected by annexin V binding (baccatin III, 46% of cells; Taxol, 36%; DMSO control, 8%) and by annexin V binding with propidium iodide uptake (baccatin III, 5% of cells; Taxol, 4% of cells; DMSO control, 1%) (not shown). From these experiments it was concluded that binding of baccatin to the Taxol binding site of microtubules is sufficient to activate the transmission of characteristic effects of Taxol in the cell lines which we had examined.

Potential Uses of the Fluorescence Anisotropy Multiwell Plate Assay in Comparison with Other Methods To Screen for Taxol Mimetics. The fluorescent method of detection of

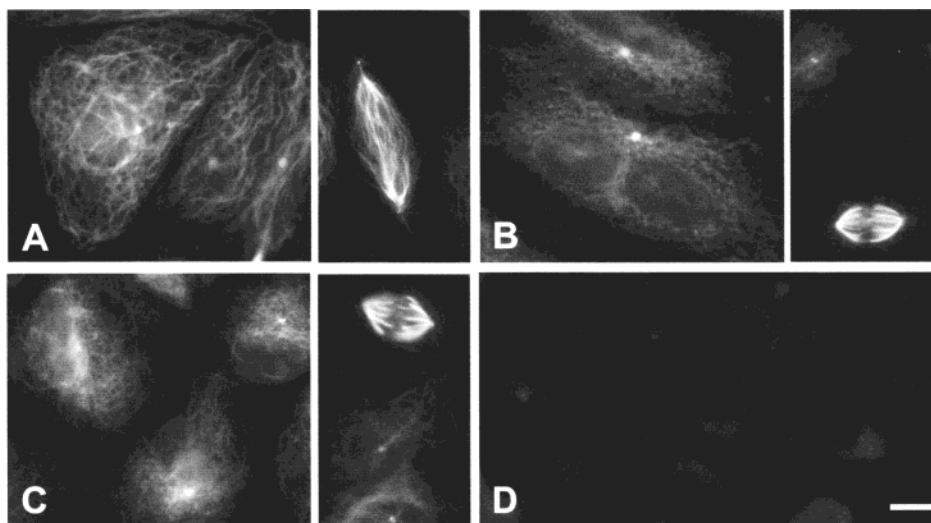


FIGURE 7: Fluorescence micrographs of microtubule cytoskeletons labeled with Flutax-2 and its displacement by baccatin III. Unfixed cytoskeletons from PtK2 cell cultures were directly imaged with 200 nM Flutax-2 under the fluorescence microscope. Panels: A, no other addition; B, with 500 nM Taxol; C, with 100 μ M baccatin III; D, with 1 mM baccatin. The bar indicates 10 μ m.

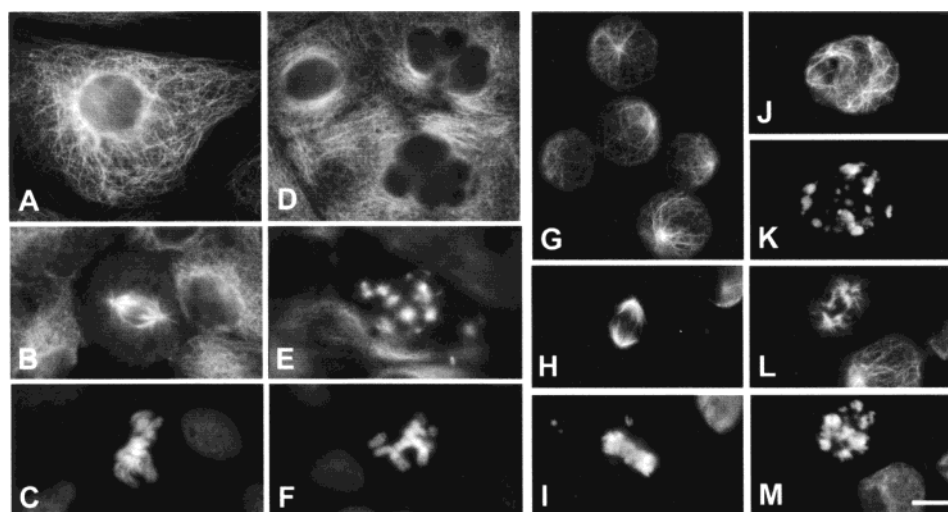


FIGURE 8: Effects of baccatin III on the microtubule cytoskeleton and mitosis of PtK2 and U937 cells. Panels: A–C are control PtK2 cells, D are cells incubated for 24 h with 0.5 mM baccatin III, E and F are cells incubated for 24 h with 0.1 mM Baccatin III, G–I are control U937 cells, and J–M are cells incubated for 17 h with 2.5 μ M baccatin III. Microtubules were stained with DM1A monoclonal antibody (A, B, D, E, G, H, J, L), and DNA was stained with Hoechst 33342 (C, F, I, K, M). The bar indicates 10 μ m.

ligand binding to the Taxol site of microtubules developed in this work constitutes a first homogeneous assay for any other substances acting on this important antitumor target. Its simplicity compares favorably with microtubule polymerization screens (3; www.cytoskeleton.com) and with the competitive assays employing radiolabeled Taxol (3, 24; Results and Figure 5 in this work). Taxane-specific monoclonal antibodies offer possibly unsurpassed sensitivity for the determination of contents of drug and closely related compounds (35–37); however, they may fail to recognize chemically unrelated ligands of the microtubule Taxol binding site. Since multiple samples can easily be analyzed with the fluorescence polarization method, this assay should be a useful tool for the evaluation of the binding affinity of newly designed compounds of the Taxol, epothilone, eleutherobin, and discodermolide families. It should also be applicable to the measurement of active Taxol-like contents of natural sources, and to high-throughput screening for new Taxol biomimetics, in a complementary fashion to cellular

screens for mitotic inhibitors, such as that employed in the discovery of monastrol (38). An interesting property of the fluorescence anisotropy assay is its sensitivity for the detection of mid affinity ligands. This is made possible by the combination of a highly fluorescent taxoid (Flutax-2) with stabilized microtubules (preserved at 4 °C), permitting the large dilution necessary for effective displacement of the probe by weaker binders, which would otherwise pass undetected. This has been exemplified by the detection of the binding of baccatin III, providing new insight into the molecular recognition of Taxol by microtubules.

While this paper was being reviewed, we have observed that the preparation of cross-linked microtubules can be improved by dialysis in cassettes (16 h, Pierce 66425) against the glycerol-containing buffer (Experimental Procedures), followed by drop-freezing into liquid nitrogen. These frozen microtubule preparations maintain upon melting their taxoid binding capacity, they give fluorescence microscopy images indistinguishable from Figure 1, and under negative stain

electron microscopy they consist of normal microtubules and open microtubule sheets (J. M. Andreu, J. F. Diaz, and I. Barasoain, unpublished results).

Contributions of the Taxane Ring System and the C-13 Side Chain to the Binding of Taxol by Microtubules. Studies of structure–activity relationship had indicated that the side chain at C-13 is an essential determinant for Taxol activity, whereas the isolated taxane ring system with its other substituents is practically inactive (11–15). On the other hand, models of the Taxol pharmacophore supported by different evidence (19–23) in combination with the electron crystallography model structure of the tubulin–Taxol complex (39) include extensive interactions of the taxane ring system and 2-*O*-benzoyl with the protein binding site, which may be considered in apparent contradiction with the activity studies. This work shows that baccatin III, a close analogue of the taxane ring system of Taxol, can replace Taxol at the microtubule binding site. Baccatin III can in fact mimic the cellular effects of Taxol (albeit with a few 100-fold lower efficiency), whereas the methyl ester of the Taxol C-13 side chain is essentially inactive. The results further reveal the role of the taxane ring system and the other substituents (C-2 benzoyl, C-4 acetyl) in Taxol binding to microtubules, which has been advanced by the finding of the biological activity of 2-*m*-azido-baccatin III by He et al. (19).

The important question arises of which are the respective contributions of the taxane ring system and the C-13 side chain to the binding of Taxol. Whereas a definitive answer in structural terms should require the eventual determination of the high-resolution structure of microtubules with bound Taxol (for review, see ref 15), the energetics of binding can be partially addressed. A simplified analysis is as follows. In our measurements, baccatin III binds to the Taxol site of microtubules with an equilibrium constant $K_b = 1.5 \times 10^5 \text{ M}^{-1}$, which translates into a binding free energy change $\Delta G_{\text{obs}} = -RT \ln K_b = -29.5 \text{ kJ mol}^{-1}$. In the same competition assay as baccatin, the value for the free energy change of binding of Taxol is $\Delta G_{\text{obs}} = -43.2 \text{ kJ mol}^{-1}$. Therefore, the increment binding free energy change which results from transforming baccatin into Taxol is $-13.7 \text{ kJ mol}^{-1}$, corresponding to the substitution of the Taxol side chain at C-13 for the 13-OH group. Assuming that the 13-OH of baccatin does not make any adventitious interaction with the protein, the binding of baccatin III may be considered equivalent to that of Taxol's taxane ring system with its other substituents.

A more rigorous comparison of the relative contributions of the taxane ring and the side chain to the affinity of Taxol binding requires that the loss of entropy of mixing of each bimolecular ligand binding reaction in dilute aqueous solution (for $A + B$ giving C , $\Delta S_m^\circ = R \ln(X_A/X_B X_C) = 33.8 \text{ J mol}^{-1} \text{ K}^{-1}$ in a 1 molal standard state) be properly accounted for, so that the standard binding free energy changes of the parts of a ligand are ideally additive (40). This is accomplished by expressing the free energy change of binding of each ligand in the unitary mole fraction standard state, $\Delta G_u^\circ = \Delta G_{\text{obs}}^\circ - 10 \text{ kJ mol}^{-1}$ (at 298 K). Thus, $\Delta G_u^\circ(\text{Taxol}) = -53.2 \text{ kJ mol}^{-1}$. Let us consider Taxol ideally equivalent to covalently linked baccatin III and the C-13 side chain, which independently bind (for the sake of simplicity) to two subsites of the Taxol binding site (see scheme in Figure 9), that is, $\Delta G_u^\circ(\text{ring system}) = \Delta G_u^\circ(\text{baccatin}) = -39.5 \text{ kJ mol}^{-1}$.

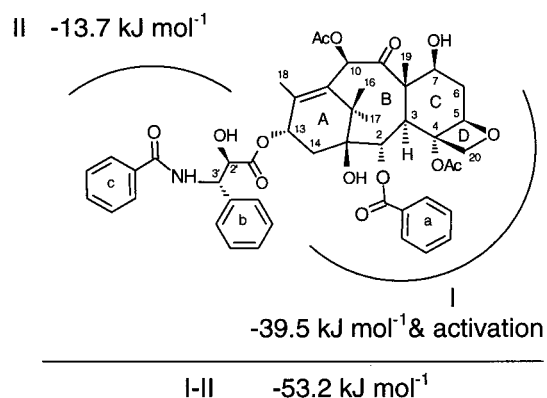


FIGURE 9: Scheme of the contributions of the taxane ring system and the C-13 side chain to the affinity of binding of Taxol to microtubules, as suggested by this work. The interaction of the taxane ring and essential substituents of Taxol with subsite I, studied with the analogue baccatin III, contributes approximately 75% of the free energy change of Taxol binding, whereas the side chain should contribute the other 25% (the binding free energy changes are expressed in the unitary mole fraction standard state so that they are additive). Occupation of subsite I by baccatin III is sufficient for tubulin activation and mimics the effects of Taxol in the cells examined.

Neglecting in a first approximation the differences in the solvation, conformation, and mobility changes between baccatin III and Taxol upon binding, it holds that $\Delta G_u^\circ(\text{side chain}) = \Delta G_u^\circ(\text{Taxol}) - \Delta G_u^\circ(\text{ring system}) = -13.7 \text{ kJ mol}^{-1}$. This analysis, though necessarily limited by its assumptions, provides very useful information. It indicates that the taxane ring system contributes roughly three-fourths and the C-13 side chain only one-fourth of the binding free energy change of Taxol (Figure 9). It predicts a free energy change of binding of the isolated side chain of $\Delta G_{\text{app}} = -3.7 \text{ kJ mol}^{-1}$, that is, an extremely weak binding with an unmeasurable equilibrium constant value $K_b = 4.5 \text{ M}^{-1}$. This is compatible with the experimental observations of inactivity in the methyl ester of the side chain ($K_b < 10^3 \text{ M}^{-1}$; Figure 4 and Results). Note, however, that the predominant conformation of Taxol in aqueous solutions is hydrophobically collapsed, involving the clustering of the 2-*O*-benzoyl, 3'-phenyl, and 4-*O*-acetyl groups (15), whereas the conformation of microtubule-bound Taxol may be different. Taking, for example, the open T–Taxol model (23), the active conformation corresponds to a minor solution conformer. The free energy change of Taxol binding which can be measured is therefore the sum of the protein–ligand contact free energy change plus the unfavorable contribution of separating the phenyl rings. Considering that the relative abundance of the T conformer in aqueous solution (J. Jimenez-Barbero and J. P. Snyder, personal communication) should be in a conservative estimation between 5% and 25% of the population, this contribution may be comprised between 7.4 and 4.0 kJ mol⁻¹. This correction applies to Taxol binding, but not to baccatin III, which needs not open in order to bind; hence, the calculated contribution of the C-13 side chain to the Taxol binding affinity should be increased by this amount. This implies that baccatin would contribute about two-thirds and the side chain one-third of the affinity of Taxol binding, which modifies a little this analysis. On the other hand, a very improbable combination of experimental errors, such as making the affinity of Taxol 10-fold higher and that of

baccatin 10-fold lower, would not qualitatively change the analysis.

In conclusion, the simplest interpretations of our results (see Figure 9) are that (i) the binding of the taxane ring system provides most of the affinity of Taxol binding, (ii) the occupancy of this part of the binding site is sufficient to turn on the transmission of the Taxol-like effects, and (iii) the binding of the side chain provides an additional anchor which, from the available evidence, is comparatively weaker. This does not preclude the binding conformation of the C-13 side chain from being quite specific, including, for example, the provision of the necessary scaffold for the essential free 2'-OH group (41) to make a hydrogen bond with a protein residue. These proposals may be tested by studying the structure–affinity relationship resulting from systematically modifying the different substituents of the Taxol molecule. At difference with the structure–activity studies, this approach pursues a quantitative description of the contribution of each part of the molecule to the affinity of binding of Taxol to microtubules.

ACKNOWLEDGMENT

We thank our colleague Dr. J. Fernando Diaz for extended help and discussions, Dr. Francisco Amat-Guerri for generously providing Flutax-2, Drs. Erkan Baloglu and David G.I. Kingston for a gift of the methyl ester of Taxol's C-13 side chain, Drs. Jesús Jimenez-Barbero, F. Amat-Guerri, and James P. Snyder for communications prior to publication, Dr. A. Ulises Acuña for criticisms, and Dr. Pedro Lastres for help with flow cytometry.

REFERENCES

- Nogales, E. (2000) *Annu. Rev. Biochem.* 69, 277–302.
- Jordan, M. A., and Wilson, L. (1998) *Curr. Opin. Cell Biol.* 10, 123–130.
- Bollag, D. M., McQueney, P. A., Zhu, J., Henses, O., Koupal, L., Liesch, J., Goetz, M., Lazarides, E., and Woods, C. M. (1995) *Cancer Res.* 55, 2325–2333.
- Ter Haar, E., Kowalsky, R. J., Lin, C. M., Longley, R. E., Gunasekera, S. P., Rosenkrantz, H. S., and Day, B. W. (1996) *Biochemistry* 35, 243–250.
- Long, B. H., Carboni, J. M., Wasserman, A. J., Cornell, L. A., Casazza, A. M., Jensen, P. R., Lindel, T., Fencal, W., and Fairchild, C. R. (1998) *Cancer Res.* 58, 1111–1115.
- Mooberry, S. L., Tien, G., Hernandez, A. H., Plubrukarn, A., and Davidson, B. S. (1999) *Cancer Res.* 59, 653–660.
- Souto, A. A., Acuña, A. U., Andreu, J. M., Barasoain, I., Abal, M., and Amat-Guerri, F. (1995) *Angew. Chem., Int. Ed. Engl.* 34, 2710–2712.
- Evangelio, J. A., Abal, M., Barasoain, I., Souto, A. A., Lillo, M. P., Acuña, A. U., Amat-Guerri, F., and Andreu, J. M. (1998) *Cell Motil. Cytoskeleton* 39, 73–90.
- Abal, M. A., Souto, A. A., Amat-Guerri, F., Acuña, A. U., Andreu, J. M., and Barasoain, I. (2001) *Cell Motil. Cytoskeleton* 49, 1–15.
- Díaz, J. F., Strobe, R., Engelborghs, Y., Souto, A. A., and Andreu, J. M. (2000) *J. Biol. Chem.* 275, 26265–26276.
- Lataste, H., Senilh, V., Wright, M., Guenard, D., and Potier, P. (1984) *Proc. Natl. Acad. Sci. U.S.A.* 81, 4090–4094.
- Kingston, D. G. I. (1994) *Trends Biotechnol.* 12, 117–125.
- Suffness, M., Ed. (1995) *Taxol, Science and Applications*, CRC Press, Boca Raton, FL.
- Kingston, D. G. I. (2000) *J. Nat. Prod.* 63, 726–734.
- Jimenez-Barbero, J., Amat-Guerri, F., and Snyder, J. P. (2001) *Curr. Med. Chem.* (in press).
- Parness, J., Kingston, D. G. I., Powell, R. G., Harracksingh, C., and Horwitz, S. B. (1982) *Biochem. Biophys. Res. Commun.* 105, 1082–1089.
- Pengsuparp, T., Kingston, D. G. I., Neidigh, K. A., Cordell, G. A., and Pezzuto, J. M. (1996) *Chem. Biol. Interact.* 101, 103–114.
- Miller, M. C., III, Johnson, K. R., Willingham M. C., and Fan, W. (1999) *Cancer Chemother. Pharmacol.* 44, 444–452.
- He, L., Jagtap, P. G., Kingston, D. G. I., Shen, H. J., Orr, G. A., and Horwitz, S. B. (2000) *Biochemistry* 39, 3972–3978.
- Rao, S., He, L., Chakravarty S., Ojima, I., Orr, G. A., and Horwitz, S. P. (1999) *J. Biol. Chem.* 274, 37990–37994.
- Li, Y., Poliks, B., Cegelski, L., Poliks, M., Gyczynski, Z., Piszcek, G., Jagtap, P. G., Studelska, D. R., Kingston, D. G. I., Schaefer, J., and Bane, S. (2000) *Biochemistry* 39, 281–291.
- Gianakakou, P., Gussio, R., Nogales, E., Downing, K. H., Zaharevitz, D., Bollbuck, B., Poy, G., Sackett, D., Nicolaou, K. C., and Fojo, T. (2000) *Proc. Natl. Acad. Sci. U.S.A.* 97, 2904–2909.
- Snyder, J. P., Nettles, J. H., Cornett, B., Downing, K. H., and Nogales, E. (2001) *Proc. Natl. Acad. Sci. U.S.A.* 98, 5321–5326.
- Diaz, J. F., and Andreu, J. M. (1993) *Biochemistry* 32, 2747–2755.
- Andreu, J. M., Perez-Ramirez, B., Gorbunoff, M. J., Ayala, D., and Timasheff, S. N. (1998) *Biochemistry* 37, 8356–8368.
- Lackowicz J. R. (1999) *Principles of fluorescence spectroscopy*, Kluwer/Plenum, New York, NY.
- Medrano, F. J., Andreu, J. M., Gorbunoff, M. J., and Timasheff, S. N. (1991) *Biochemistry* 30, 3770–3777.
- De Inés, C., Leynadier, D., Barasoain, I., Peyrot, V., Garcia, P., Briand, C., Renner, G. A., and Temple, C., Jr. (1994) *Cancer Res.* 54, 75–84.
- Martin, S., Reutelingsperger, C. P. M., McGahon, A. J., Rader, J. A., Van Schie, R. C., La Face, D. M., and Green, D. R. (1995) *J. Exp. Med.* 182, 1545–1556.
- Nogales, E., Whittaker, M., Milligan, R. A., and Downing, K. H. (1999) *Cell* 96, 79–88.
- Parness, J., and Horwitz, S. B. (1981) *J. Cell Biol.* 91, 479–487.
- Han, Y., Chaudhary, A. G., Chordia, M. D., Sackett, D. L., Perez-Ramirez, B., Kingston, D. G., and Bane, S. (1996) *Biochemistry* 35, 14173–14183.
- Li, Y., Edsall, R., Jr., Jagtap, P. G., Kingston, D. G. I., and Bane, S. (2000) *Biochemistry* 39, 616–623.
- Chatterjee S., Barron, D., Vos, S., and Bane, S. (2001) *Biochemistry* 40, 6964–6970.
- Grothaus, P. G., Bignami, G. S., O'Malley, S., Harada, K. E., Byrnes, J. B., Waller, D. F., Raybould, T. J., McGuire, M. T., and Alvarado, B. (1995) *J. Nat. Prod.* 58, 1003–1014.
- O'Boyle, K. P., Wang, Y., Schwarz, E. L., Regl, D. L., Einzig, A., Dutcher, J. P., Wiernik, P. H., and Horwitz, S. B. (1997) *Cancer* 79, 1022–1030.
- Bicamumpaka, C., and Page, M. (1998) *J. Immunol. Methods* 212, 1–7.
- Mayer, T. U., Kapoor, T. M., Haggarty, S. J., King, R. W., Schreiber, S. L., and Mitchison, T. J. (1999) *Science* 286, 971–974.
- Nogales, E., Wolf, S. G., and Downing, K. (1998) *Nature* 391, 199–203.
- Andreu, J. M., and Timasheff, S. N. (1982) *Biochemistry* 21, 534–543.
- Jimenez-Barbero, J., Souto, A. A., Abal, M., Barasoain, I., Evangelio, J. A., Acuña, A. U., Andreu, J. M., and Amat-Guerri, F. (1998) *Bioorg. Med. Chem.* 6, 1857–1863.

BI010869+